

Sulfonate-Grafted Porous Polymer Networks for Preferential CO₂ Adsorption at Low Pressure

Weigang Lu,[†] Daqiang Yuan,[†] Julian Sculley,[†] Dan Zhao,[‡] Rajamani Krishna,[§] and Hong-Cai Zhou^{*†}

[†]Department of Chemistry, Texas A&M University, College Station, Texas 77842, United States

[‡]Chemical Sciences and Engineering Division, Argonne National Laboratory, Argonne, Illinois 60439, United States

[§]Van't Hoff Institute for Molecular Sciences, University of Amsterdam, Science Park 904, 1098 XH Amsterdam, The Netherlands

S Supporting Information

ABSTRACT: A porous polymer network (PPN) grafted with sulfonic acid (PPN-6-SO₃H) and its lithium salt (PPN-6-SO₃Li) exhibit significant increases in isosteric heats of CO₂ adsorption and CO₂-uptake capacities. IAST calculations using single-component-isotherm data and a 15/85 CO₂/N₂ ratio at 295 K and 1 bar revealed that the sulfonate-grafted PPN-6 networks show exceptionally high adsorption selectivity for CO₂ over N₂ (155 and 414 for PPN-6-SO₃H and PPN-6-SO₃Li, respectively). Since these PPNs also possess ultrahigh physicochemical stability, practical applications in postcombustion capture of CO₂ lie well within the realm of possibility.

One of the primary scientific discussions currently ongoing is that of global climate change, which is at least in part attributed to the increasing CO₂ concentration in the air. Carbon capture and sequestration (CCS), a process to separate CO₂ from flue gas, has been proposed as a feasible way to mediate the atmospheric CO₂ concentration. Conventional CO₂ capture processes employed in power plants worldwide are postcombustion “wet scrubbing” methods involving chemical adsorption of CO₂ by amine solutions such as monoethanolamine (MEA). There are several disadvantages with wet scrubbing, including the considerable parasitic power consumption involved in the regeneration of the solutions and the measures that must be taken to control the corrosive solutions, both of which lead to reduced efficiencies and increased costs for electricity generation.¹

An alternative, energy-conserving approach involves the use of porous materials, which can easily take up and release CO₂ through a physisorption mechanism. Recently, metal–organic frameworks (MOFs), adsorbents made of metal ions and organic linkers with high surface areas and tunable pore sizes, have emerged to show remarkable CO₂-uptake capacities and CO₂/N₂ selectivities at room temperature.² However, the majority of MOFs have difficulty in meeting the stringent industrial requirements.³ On the other hand, purely organic porous polymers, another class of adsorbents with comparable surface areas and pore sizes, exhibit much higher physicochemical stability as a result of the covalent bonding nature of the network construction.⁴ Despite the fact that most of them are amorphous, their stability is desirable in practical applications.

Besides physicochemical stability, high CO₂-uptake capacity and CO₂/N₂ selectivity under ambient conditions are equally

essential for porous materials to be industrially applicable. Presumably, increasing the isosteric heat of CO₂ adsorption through the introduction of CO₂-philic moieties should have a great influence on both. Indeed, significant increases of isosteric heats and CO₂/N₂ adsorption selectivity have been observed upon pre- or postsynthetic introduction of polar functionalities;⁵ however, this approach usually has a negative impact on the surface area that can lead to very low CO₂-uptake capacity if the surface area is severely compromised. One possible strategy to tackle this issue is to judiciously select porous polymers with ultrahigh surface areas and physicochemical stability as starting materials. Therefore, sufficient surface area can be retained after the introduction of CO₂-philic moieties.

Herein we report the synthesis of PPN-6, a porous polymer network (PPN) with permanent porosity, and grafting of PPN-6 with sulfonic acid and lithium sulfonate. The resulting PPN-6-SO₃H and PPN-6-SO₃Li materials showed significant increases in CO₂-uptake capacities and exceptionally large CO₂/N₂ adsorption selectivities under ambient conditions.

PPN-6 (also known as PAF-1^{4a}) was synthesized by an optimized Yamamoto homocoupling reaction⁶ using tetrakis(4-bromophenyl)methane. The default diamondoid framework topology imposed by the tetrahedral monomers provides widely open and interconnected pores that efficiently prevent the formation of “dead space”;^{4b} more importantly, the extremely robust all-carbon scaffold of the network makes it ideal for attachment of polar functionalities on biphenyl species under harsh reaction conditions. By reaction with chlorosulfonic acid, PPN-6 was modified to give PPN-6-SO₃H, which was further neutralized to produce PPN-6-SO₃Li (Scheme 1).

Nitrogen gas adsorption/desorption isotherms of the three networks were collected at 77 K [Figure S1a in the Supporting Information (SI)]. Notably, the large desorption hysteresis in PPN-6 disappeared and almost ideal type-I isotherms were obtained for sulfonate-grafted PPN-6. The Brunauer–Emmett–Teller (BET) surface areas obtained from the experimental data were 4023, 1254, and 1186 m² g⁻¹ for PPN-6, PPN-6-SO₃H, and PPN-6-SO₃Li, respectively (Figures S2–S4). As expected, the surface area decreased upon functionalization. The pore size distributions of the three networks were derived using the entire range of the N₂ adsorption isotherms measured at 77 K. Along with the decrease in surface area, the pore size became progressively smaller with aromatic sulfonation and ensuing lithiation (Figure S1b).

Received: September 17, 2011

Published: October 18, 2011

Scheme 1. Synthesis and Grafting of PPN-6

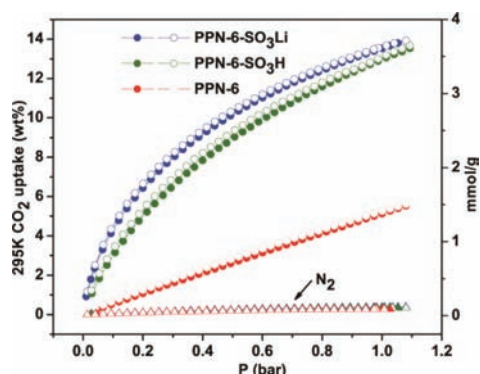
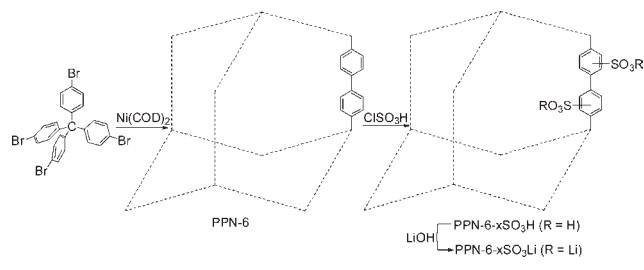


Figure 1. Gravimetric CO_2 and N_2 adsorption (●)/desorption (○) isotherms at 295 K (see the SI for magnified N_2 isotherm curves).

Recent studies have revealed that one of the desirable features for enhancing the CO_2 -uptake capacity at ambient temperature is a suitable pore size commensurate with the kinetic diameter of a CO_2 molecule.⁷ The relatively small pore sizes of both sulfonate-grafted PPN-6 networks fall into the 5.0–10.0 Å range, which is believed to be suitable for CO_2 uptake and thus for CO_2 separation from other gases with relatively larger kinetic diameters, such as N_2 and CH_4 .

Strong interactions between the network and CO_2 are another desirable feature for enhancing the CO_2 -uptake capacity. Functionalization of all-carbon-scaffold networks can be expected to create electric fields on the surface that impart to the networks a strong affinity toward CO_2 through its high quadrupole moment. Indeed, the sulfonate-grafted PPN-6 materials displayed significantly enhanced CO_2 -uptake capacities. As shown in Figure 1, nongrafted PPN-6 has a gravimetric CO_2 uptake of 5.1 wt % at 295 K and 1 bar, whereas sulfonate-grafted PPN-6 showed remarkable increases in gravimetric CO_2 uptake, with values of 13.1 and 13.5 wt % (equivalent to 3.6 and 3.7 mmol g^{-1}) for PPN-6- SO_3H and PPN-6- SO_3Li , respectively. To the best of our knowledge, the values are the highest among all microporous organic polymers reported to date.⁸ The surge in volumetric uptake with sulfonate grafting is even more significant, from 8.1 g L^{-1} for PPN-6 to 52.5 g L^{-1} for PPN-6- SO_3H and 79.9 g L^{-1} for PPN-6- SO_3Li (Figure S5; the tap densities of the three networks used to calculate the volumetric capacities were measured to be 0.15, 0.35, and 0.51 g cm^{-3} , respectively). Relative to PPN-6- SO_3H , the initial CO_2 uptake for PPN-6- SO_3Li is more pronounced; the Li^+ cation in $-\text{SO}_3\text{Li}$ has up to three open coordination sites after full activation, which results in stronger interactions with CO_2 molecules.⁹

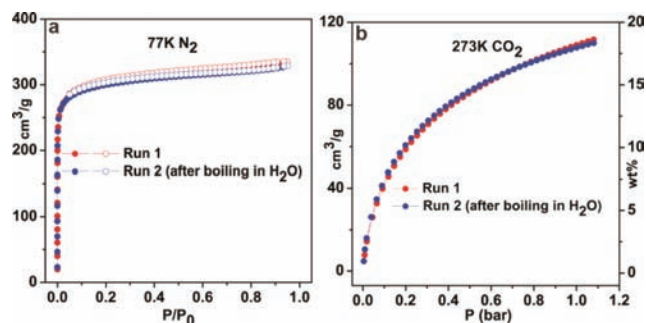


Figure 2. (a) N_2 adsorption (●)/desorption (○) isotherms of PPN-6- SO_3Li at 77 K. (b) Gravimetric CO_2 adsorption curves for PPN-6- SO_3Li at 273 K. Run 2 employed material regenerated after run 1 by boiling in water for 6 h.

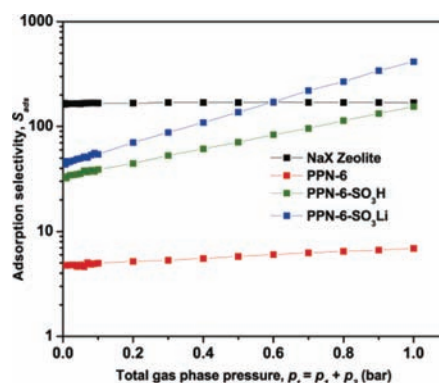


Figure 3. IAST-predicted adsorption selectivities for PPN-6 (red), PPN-6- SO_3H (green), PPN-6- SO_3Li (blue), and NaX zeolite (black).

These two sulfonate-grafted PPNs showed no obvious loss of surface area or decrease in CO_2 -uptake capacity even after being boiled in water for 6 h (Figure 2 and Figure S8). Since they were synthesized in highly corrosive acid (ClSO_3H) and/or base (LiOH) solution, we can be confident of their ultrahigh physicochemical stability.

Aside from high CO_2 -uptake capacity and physicochemical stability, high selectivity for CO_2 over N_2 under ambient conditions is another prerequisite for industrial CO_2 capture applications. The ideal adsorption solution theory (IAST) of Myers and Prausnitz¹⁰ has been reported to predict binary gas mixture adsorption in many porous materials accurately.¹¹ To judge the merit of the sulfonate groups for CO_2/N_2 separation, the adsorption selectivities [defined as $S_{\text{ads}} = (q_1/q_2)/(p_1/p_2)$, where q_i is the amount of i adsorbed and p_i is the partial pressure of i in the mixture] of the three networks for CO_2 over N_2 in flue-gas streams (typically 15% CO_2 and 85% N_2) were estimated from the experimental single-component isotherms. Sulfonate-grafted PPN-6 exhibited exceptionally high adsorption selectivity for CO_2 over N_2 at 295 K and 1 bar ($S_{\text{ads}} = 150$ for PPN-6- SO_3H and 414 for PPN-6- SO_3Li). As shown in Figure 3, the selectivities of sulfonate-grafted PPN-6 are comparable to that of NaX zeolite, which was calculated with the same parameters using the experimental isotherm data of Belmabkhout et al.¹² and Cavenati et al.¹³ Thus, these materials hold considerable promise for postcombustion carbon capture applications. To understand the hierarchy of adsorption selectivity, we note that the calculated pore volumes for PPN-6, PPN-6- SO_3H , and PPN-6- SO_3Li are

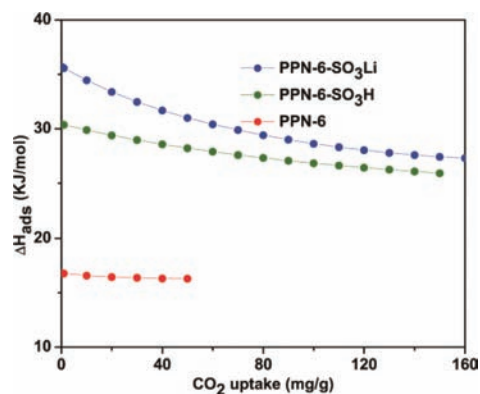


Figure 4. Isosteric heats of adsorption, as calculated from the adsorption curves at three different temperatures: PPN-6 (red); PPN-6-SO₃H (green); PPN-6-SO₃Li (blue).

2.44, 0.58, and 0.52 cm³ g⁻¹ respectively. The largest adsorption selectivity in favor of CO₂ is obtained with PPN-6-SO₃Li, which has the smallest pore volume.

It is worth noting that high CO₂-uptake capacity at 1 bar does not necessarily lead to a large selectivity for CO₂ over other components of a gas mixture, particularly for low-pressure post-combustion applications where the flue gas usually contains ~15% CO₂. Thus, a large uptake capacity for CO₂ at 0.15 bar (the partial pressure of CO₂ in flue gas) is more relevant to realistic postcombustion applications. The mass of CO₂ taken up at 0.15 bar divided by the mass of N₂ taken up at 0.75 bar is often used to evaluate CO₂/N₂ selectivity. The calculated selectivity jumps from 3.0 for PPN-6 to 15 for PPN-6-SO₃H to 17 for PPN-6-SO₃Li (Table S2); these values compare well to those other porous materials with high performance, such as metal-loaded MOF-253 (selectivity = 12).¹⁴

At 295 K and 0.15 bar, the CO₂-uptake capacity of PPN-6-SO₃Li is 5.4 wt %. This value is close to the working capacity of 30% MEA solution, which is frequently reported as 5.5 wt %.¹⁵ Notably, the CO₂ sorption isotherms of sulfonate-grafted PPNs are virtually reversible, which indicates a lower generation cost in comparison with MEA solution.

To provide a better understanding of the adsorption properties, the isosteric heats of adsorption were calculated from the CO₂ adsorption isotherms at three different temperatures (Figure 4 and Figures S11–S13). As expected, at zero-loading, PPN-6-SO₃H and PPN-6-SO₃Li showed heats of adsorption reaching 30.4 and 35.7 kJ mol⁻¹, respectively, which are substantially higher than that of nongrafted PPN-6 (17 kJ mol⁻¹). Another acid-functionalized porous polymer (CMP-1-COOH) with similar heat of adsorption (32.6 kJ mol⁻¹) has been reported recently.¹⁶ In both cases, the heats of adsorption are much higher than those of the nonpolar, unfunctionalized analogues. The increase for PPN-6-SO₃H is larger than that for CMP-1-COOH, possibly because of the relatively smaller pore size of CMP-1 than PPN-6. Small pore size has been reported to increase the heat of adsorption.¹⁷ The salt PPN-6-SO₃Li has an isosteric heat of adsorption that is even higher. The trend is consistent with computational studies suggesting that polar functionalities are effective in increasing the heat of adsorption for CO₂.^{5c,9,18} The discrepancy between PPN-6-SO₃H and PPN-6-SO₃Li can be largely attributed to stronger electrostatic interactions between CO₂ and the Li⁺ cations.

The general understanding is that the CO₂-uptake capacity is dictated by many factors, such as surface area, pore functionality, pore size, etc., with each factor carrying different weights at various pressures and temperatures. At very low pressures, the interactions between CO₂ and the pore surface play the dominant role for CO₂ uptake. This appears to be the case for both sulfonate-grafted PPNs, as is most evident in the high heats of adsorption. However, as the pressure is increased to 1 bar, the effect of functionality gradually weakens, and the influence of surface area progressively weighs in, consistent with the decrease of the heat of adsorption.

The foregoing results demonstrate that aromatic sulfonation and ensuing lithiation result in significant enhancements of the CO₂-uptake capacity and CO₂/N₂ adsorption selectivity under ambient conditions. Given the outstanding physicochemical stability, these materials might find practical applications in postcombustion CO₂ capture. To improve the CO₂-uptake capacity and CO₂/N₂ selectivity further with this strategy, using porous materials with even higher surface areas as starting materials^{4a,f} should have great potential. In addition, uniformly large pores would be ideal for shuttling the reactants and improving the diffusion rates. Moreover, much stronger CO₂-philic moieties, such as alkylamine groups, would be more effective in increasing the heat of adsorption.^{15a,19} Work on further expansion of this series of materials along these lines is currently underway in our lab.

■ ASSOCIATED CONTENT

S Supporting Information. Detailed experimental procedures, elemental analysis results, FT-IR and solid-state NMR spectra, SEM images, additional gas sorption isotherms, and details of the IAST calculations. This material is available free of charge via the Internet at <http://pubs.acs.org>.

■ AUTHOR INFORMATION

Corresponding Author

zhou@mail.chem.tamu.edu

■ ACKNOWLEDGMENT

This work was supported by the U.S. Department of Energy (DE-SC0001015, DE-FC36-07GO17033, and DE-AR0000073), the National Science Foundation (CBET-0930079), and the Welch Foundation (A-1725). We acknowledge Dr. Vladimir Bakhmoutov for his help with solid-state NMR spectroscopy and Dr. Michael Pendleton for his help with the SEM images.

■ REFERENCES

- (1) (a) *Carbon Dioxide Chemistry: Environmental Issues*; Pradier, J. P. C.-M., Ed.; Royal Society of Chemistry: Cambridge, U.K., 1994. (b) MacDowell, N.; Florin, N.; Buchard, A.; Hallett, J.; Galindo, A.; Jackson, G.; Adjiman, C. S.; Williams, C. K.; Shah, N.; Fennell, P. *Energy Environ. Sci.* **2010**, *3*, 1645. (c) D'Alessandro, D. M.; McDonald, T. *Pure Appl. Chem.* **2011**, *83*, 57. (d) Hao, G. P.; Li, W. C.; Lu, A. H. *J. Mater. Chem.* **2011**, *21*, 6447. (e) Wang, Q. A.; Luo, J. Z.; Zhong, Z. Y.; Borgna, A. *Energy Environ. Sci.* **2011**, *4*, 42.
- (2) (a) Li, J.-R.; Ma, Y.; McCarthy, M. C.; Sculley, J.; Yu, J.; Jeong, H.-K.; Balbuena, P. B.; Zhou, H.-C. *Coord. Chem. Rev.* **2011**, *255*, 1791. (b) Mason, J. A.; Sumida, K.; Herm, Z. R.; Krishna, R.; Long, J. R. *Energy Environ. Sci.* **2011**, *4*, 3030.

(3) (a) D'Alessandro, D. M.; Smit, B.; Long, J. R. *Angew. Chem., Int. Ed.* **2010**, *49*, 6058. (b) Keskin, S.; van Heest, T. M.; Sholl, D. S. *ChemSusChem* **2010**, *3*, 879.

(4) (a) Ben, T.; Ren, H.; Ma, S. Q.; Cao, D. P.; Lan, J. H.; Jing, X. F.; Wang, W. C.; Xu, J.; Deng, F.; Simmons, J. M.; Qiu, S. L.; Zhu, G. S. *Angew. Chem., Int. Ed.* **2009**, *48*, 9457. (b) Lu, W. G.; Yuan, D. Q.; Zhao, D.; Schilling, C. L.; Plietzsch, O.; Muller, T.; Brase, S.; Guenther, J.; Blumel, J.; Krishna, R.; Li, Z.; Zhou, H. C. *Chem. Mater.* **2010**, *22*, 5964. (c) Dawson, R.; Laybourn, A.; Khimiyak, Y. Z.; Adams, D. J.; Cooper, A. I. *Macromolecules* **2010**, *43*, 8524. (d) Holst, J. R.; Stockel, E.; Adams, D. J.; Cooper, A. I. *Macromolecules* **2010**, *43*, 8531. (e) Rabbani, M. G.; El-Kaderi, H. M. *Chem. Mater.* **2011**, *23*, 1650. (f) Yuan, D.; Lu, W.; Zhao, D.; Zhou, H.-C. *Adv. Mater.* **2011**, *23*, 3723. (g) Jiang, J.-X.; Su, F.; Trewin, A.; Wood, C. D.; Campbell, N. L.; Niu, H.; Dickinson, C.; Ganin, A. Y.; Rosseinsky, M. J.; Khimiyak, Y. Z.; Cooper, A. I. *Angew. Chem., Int. Ed.* **2007**, *46*, 8574. (h) Rose, M.; Bohlmann, W.; Sabo, M.; Kaskel, S. *Chem. Commun.* **2008**, 2462. (i) Germain, J.; Fréchet, J. M. J.; Svec, F. *Small* **2009**, *5*, 1098. (j) Germain, J.; Fréchet, J. M. J.; Svec, F. *Chem. Commun.* **2009**, 1526. (k) Yuan, S.; Dorney, B.; White, D.; Kirklin, S.; Zapol, P.; Yu, L.; Liu, D.-J. *Chem. Commun.* **2010**, *46*, 4547. (l) Xia, J.; Yuan, S.; Wang, Z.; Kirklin, S.; Dorney, B.; Liu, D.-J.; Yu, L. *Macromolecules* **2010**, *43*, 3325.

(5) (a) Dawson, R.; Adams, D. J.; Cooper, A. I. *Chem. Sci.* **2011**, *2*, 1173. (b) Demessence, A.; D'Alessandro, D. M.; Foo, M. L.; Long, J. R. *J. Am. Chem. Soc.* **2009**, *131*, 8784. (c) Torrisi, A.; Bell, R. G.; Mellot-Draznieks, C. *Cryst. Growth Des.* **2010**, *10*, 2839.

(6) Schmidt, J.; Werner, M.; Thomas, A. *Macromolecules* **2009**, *42*, 4426.

(7) Zheng, S. T.; Bu, J. T.; Li, Y. F.; Wu, T.; Zuo, F.; Feng, P. Y.; Bu, X. H. *J. Am. Chem. Soc.* **2010**, *132*, 17062.

(8) (a) Dawson, R.; Stockel, E.; Holst, J. R.; Adams, D. J.; Cooper, A. I. *Energy Environ. Sci.* **2011**, *4*, 4239. (b) Rabbani, M. G.; El-Kaderi, H. M. *Chem. Mater.* **2011**, *23*, 1650.

(9) Xu, Q.; Liu, D. H.; Yang, Q. Y.; Zhong, C. L.; Mi, J. G. *J. Mater. Chem.* **2010**, *20*, 706.

(10) Myers, A. L.; Prausnitz, J. M. *AIChE J.* **1965**, *11*, 121.

(11) (a) Bae, Y. S.; Farha, O. K.; Hupp, J. T.; Snurr, R. Q. *J. Mater. Chem.* **2009**, *19*, 2131. (b) Yazaydin, A. O.; Benin, A. I.; Faheem, S. A.; Jakubczak, P.; Low, J. J.; Willis, R. R.; Snurr, R. Q. *Chem. Mater.* **2009**, *21*, 1425. (c) Zheng, B. S.; Bai, J. F.; Duan, J. G.; Wojtas, L.; Zaworotko, M. J. *J. Am. Chem. Soc.* **2011**, *133*, 748. (d) Simmons, J. M.; Wu, H.; Zhou, W.; Yildirim, T. *Energy Environ. Sci.* **2011**, *4*, 2177. (e) Krishna, R.; van Baten, J. M. *Phys. Chem. Chem. Phys.* **2011**, *13*, 10593. (f) Belmabkhout, Y.; Sayari, A. *Adsorption* **2009**, *15*, 318. (g) Goj, A.; Sholl, D. S.; Akten, E. D.; Kohen, D. *J. Phys. Chem. B* **2002**, *106*, 8367.

(12) Belmabkhout, Y.; Pirngruber, G.; Jolimaître, E.; Methivier, A. *Adsorption* **2007**, *13*, 341.

(13) Cavenati, S.; Grande, C. A.; Rodrigues, A. E. *J. Chem. Eng. Data* **2004**, *49*, 1095.

(14) Bloch, E. D.; Britt, D.; Lee, C.; Doonan, C. J.; Uribe-Romo, F. J.; Furukawa, H.; Long, J. R.; Yaghi, O. M. *J. Am. Chem. Soc.* **2010**, *132*, 14382.

(15) (a) McDonald, T. M.; D'Alessandro, D. M.; Krishna, R.; Long, J. R. *Chem. Sci.* **2011**, *2*, 2022. (b) Peeters, A. N. M.; Faaij, A. P. C.; Turkenburg, W. C. *Int. J. Greenhouse Gas Control* **2007**, *1*, 396.

(16) Dawson, R.; Adams, D. J.; Cooper, A. I. *Chem. Sci.* **2011**, *2*, 1173.

(17) An, J.; Rosi, N. L. *J. Am. Chem. Soc.* **2010**, *132*, 5578.

(18) (a) Babarao, R.; Dai, S.; Jiang, D. E. *Langmuir* **2011**, *27*, 3451. (b) Liu, B.; Smit, B. *Langmuir* **2009**, *25*, 5918. (c) Wu, D.; Xu, Q.; Liu, D. H.; Zhong, C. L. *J. Phys. Chem. C* **2010**, *114*, 16611.

(19) (a) Arstad, B.; Fjellvag, H.; Kongshaug, K. O.; Swang, O.; Blom, R. *Adsorption* **2008**, *14*, 755. (b) Jin, Y. H.; Voss, B. A.; Jin, A.; Long, H.; Noble, R. D.; Zhang, W. *J. Am. Chem. Soc.* **2011**, *133*, 6650.